Article

Modified *Urtica dioica* Leaves as a Low-Cost and Effective Adsorbent for the Simultaneous Removal of Pb(II), Cu(II), Cd(II), and Zn(II) from Aqueous Solution

Enkhtuul Mendsaikhan [1,2], Munkhpurev Bat-Amgalan [2], Ganchimeg Yunden [2], Naoto Miyamoto [3], Naoki Kano [3,*] and Hee Joon Kim [4]

1   Graduate School of Science and Technology, Niigata University, 8050 Ikarashi 2-Nocho, Nishi-ku, Niigata 950-2181, Japan; f22k503k@mail.cc.niigata-u.ac.jp
2   Department of Chemical Engineering, School of Applied Sciences, Mongolian University of Science and Technology, 8th khoroo, Baga Toiruu 34, Sukhbaatar District, Ulaanbaatar 14191, Mongolia; munkhpurev@must.edu.mn (M.B.-A.); ganchimeg.yu@must.edu.mn (G.Y.)
3   Department of Chemistry and Chemical Engineering, Faculty of Engineering, Niigata University, 8050 Ikarashi 2-Nocho, Nishi-ku, Niigata 950-2181, Japan; nmiyamoto@eng.niigata-u.ac.jp
4   Department of Environmental Chemistry and Chemical Engineering, School of Advanced Engineering, Kogakuin University, 2665-1 Nakano, Tokyo 192-0015, Japan; kim@cc.kogakuin.ac.jp
*   Correspondence: kano@eng.niigata-u.ac.jp; Tel.: +81-025-262-7218

Abstract: This study investigates the simultaneous adsorption of Pb(II), Cu(II), Cd(II), and Zn(II) ions from aqueous solutions using *Urtica dioica* leaves (UDLs) modified with sulfuric acid, followed by heat treatment to enhance adsorptive properties. The heat treatment significantly increased the adsorbent's specific surface area to 451.93 $m^2 \cdot g^{-1}$. Batch adsorption experiments were performed to determine the influence of the contact time, pH of the aqueous solution, adsorbent dosage, temperature, and initial metal concentration on the adsorption efficiency. The material (modified UDLs) was characterized using X-ray diffraction (XRD), Fourier transform infrared spectroscopy (FT-IR), scanning electron microscope (SEM), and X-ray photoelectron spectroscopy (XPS). Maximum removal efficiencies were determined as 99.2%, 96.4%, 88.7%, and 83.6% for Pb(II), Cu(II), Cd(II), and Zn(II) ions, respectively. Adsorption isotherms and kinetics revealed that the process follows the Langmuir equation and pseudo-second-order models, indicating monolayer adsorption and chemisorption mechanisms. Furthermore, thermodynamic analysis indicated that the adsorption processes are spontaneous and endothermic in nature. The influence of competing ions on the adsorption of multiple heavy metals was also discussed. The results suggest that sulfuric acid and heat-treated *Urtica dioica* leaves can offer a promising, low-cost, and eco-friendly adsorbent for removing heavy metal ions from contaminated water.

Keywords: *Urtica dioica* leaves (UDLs); multi-component heavy metals; removal efficiency; wastewater treatment; low-cost adsorbent

1. Introduction

Water pollution caused by heavy metals has become a major environmental issue in recent years. Various industrial activities, including mining, electroplating, leather tanning, metal processing, steel metallurgy, pigment synthesis and dyeing, and battery production, release heavy metals into aquatic ecosystems [1–3]. Lead (Pb(II)), copper (Cu(II)), cadmium (Cd(II)), and zinc (Zn(II)) are some of the most common heavy metal pollutants found in industrial wastewater [4,5]. They are non-biodegradable and toxic pollutants that can

accumulate in living organisms and the environment, leading to severe health problems like neurological, cardiovascular, carcinogenic, kidney, blood, nervous, and bone diseases [5–7]. Although numerous technologies, including chemical precipitation, ion exchange, ultrafiltration, reverse osmosis, membrane, and adsorption, have been employed to remove heavy metals from industrial wastewater, many developing countries find these modern solutions financially inaccessible [8–12]. Intending to combat these issues, research efforts have increased to develop an efficient, eco-friendly, and low-cost adsorbent to treat wastewater. Adsorbents can be used naturally or prepared in multiple ways [13]. Generally, many materials, such as activated carbon, different clays, polymeric materials, nanocomposites, and natural adsorbents, are used for adsorption [14,15]. Natural adsorbents such as various plant leaves [16–18], roots, seeds, tree barks, coconut shells, eggshells [19], tea, and agricultural wastes [13,20] have advantages such as very low costs compared to other adsorbents, are grown in many areas in nature, are easily supplied, are considered to produce zero waste, have a relatively high surface area, and have many functional groups [21]. Over the years, various methods including mechanical, thermal, and chemical treatments have been developed to enhance the adsorption capabilities of lignocellulosic biomass, broadening their applicability in heavy metal separation processes [22–24]. Sulfuric acid modification is well-suited for enhancing adsorbents because it effectively alters the chemical and structural properties of biomass, significantly boosting its adsorption capabilities. Additionally, sulfuric acid is an inexpensive reagent, making it a cost-effective choice for large-scale applications [25,26]. So far, we have studied some materials to enhance the adsorption capacity of heavy metals [27–31]. In this study, we chemically modified *Urtica dioica* leaves (UDLs) using sulfuric acid. Furthermore, these chemically modified UDLs underwent thermal treatment to produce the final adsorbent material with enhanced adsorption properties.

Urtica dioica, usually called common nettle, belongs to the Urticaceae family and grows worldwide, with the ability to grow 1 to 2 m. The main components of *Urtica dioica* are cellulose (80.1–90.4%), hemicellulose (5.6–9.5%), and lignin (1.4–4.4%) [32]. These constituents have potential functional groups, such as hydroxyl, carbonyl, amino, carboxylic, and alkoxyl, with good affinities for metal ions. Likewise, *Urtica dioica* has a significant adsorption potential, as it is soft, resistant, and has a low specific weight. In the literature, it is also known that this plant is used for phytoremediation [33,34]. In several studies, the authors used *Urtica dioica* as a low-cost adsorbent for removing pollutants from an aqueous solution [35–38]. Moreover, it was found that chemically treated biomass adsorbents exhibit significantly higher adsorption capacities compared to untreated ones [39]. Abundant natural materials have the potential to be used as inexpensive sorbents. Furthermore, when these materials reach the end of their lifetime, they can be disposed of without needing costly regeneration.

Polluted effluent water, with concentrations above the regulated limit, contains a myriad of metal ions and, as such, mono- or bi-adsorption systems are not realistic; hence, simultaneous multi-metal adsorption systems [40,41] are needed. The concentration range of 50–500 mg/L of for Pb(II), Cu(II), Cd(II), and Zn(II) chosen in this work can be found in untreated industrial wastewater, such as from mining, battery manufacturing, electronics recycling, and metal finishing [42,43]. Altering the ratios of metal ions in solution can significantly impact adsorption behavior due to competition for active sites on the adsorbent. For instance, in a study examining the competitive adsorption of Cd^{2+}, Pb^{2+}, and Cu^{2+} ions using a multigroup-functionalized cellulose adsorbent, it was observed that Cu^{2+} exhibited the strongest inhibitory effect on the adsorption of the other metals. This indicates that higher concentrations of Cu^{2+} can suppress the adsorption of Cd^{2+} and Pb^{2+} [44]. In our study, the chosen metal ion ratios reflect typical mixtures in industrial wastewater, allowing the observation of competitive adsorption between metals. The present research

is focused on the behavior of modified *Urtica dioica* leaves regarding multi-component heavy metals Pb(II), Cu(II), Cd(II), and Zn(II), evaluating different parameters in the system, such as pH, particle size, biosorbent dosage, time, and metal ion concentration. The removal efficiency of the multi-metal ion mixtures was discussed. The characterization of the adsorbents was performed using Fourier transform infrared spectroscopy (FTIR), X-ray photoelectron spectroscopy (XPS), scanning electron microscopy (SEM-EDS), and X-ray diffraction (XRD) analyses. The equilibrium data were fitted to Langmuir and Freundlich isotherm models, while the kinetics data were correlated according to typical kinetics models (pseudo-first-order and pseudo-second-order model).

The main original points in this paper are (1) effectively utilizing *Urtica dioica* leaves as a low-cost and eco-friendly adsorbent for the simultaneous removal of multi-component heavy metals, and (2) determining the activation energy (not only thermodynamic parameters such as ΔG^0, ΔH^0, and ΔS^0) to quantify the energy barrier of the adsorption process.

2. Results and Discussion

2.1. Characterizations of Materials

2.1.1. SEM-EDS Analysis

SEM images for unmodified UDLs (a), H_2SO_4-modified UDLs (b), and H_2SO_4-modified UDLs after adsorption (c) along with TUDL500 (d,e) are presented in Figure 1. To enhance imaging, the samples were coated with a thin layer of gold. As shown in Figure 1a, unmodified UDLs had a rough and irregular surface structure. Figure 1b shows the increased surface roughness and the appearance of micropores, which improve adsorption properties. After the adsorption of heavy metals, the interaction of H_2SO_4-modified UDLs with heavy metals resulted in the formation of white, shiny deposits on its surface, as illustrated in Figure 1c. The SEM image after heat treatment (Figure 1d) reveals a significant increase in porosity, with interconnected pores forming a network. It is suggested that this structure enhances adsorption capacity by increasing the surface area. Figure 1e reveals a highly porous structure, a characteristic feature retained from the pyrolysis process. However, many of the visible pores in the image are partially filled, providing direct evidence of heavy metal ion adsorption. The EDS analysis is presented in the Supplementary Information (Figure S3a–c).
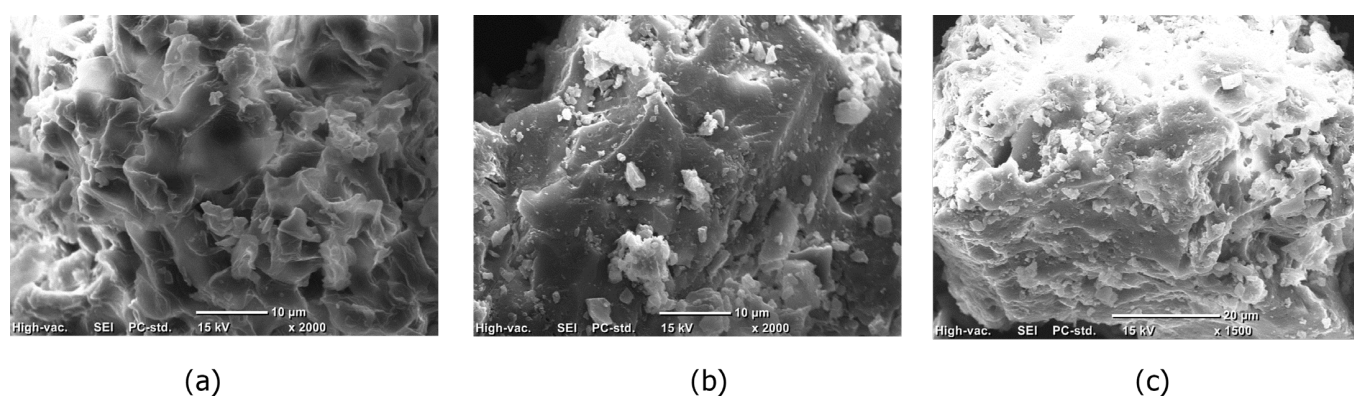

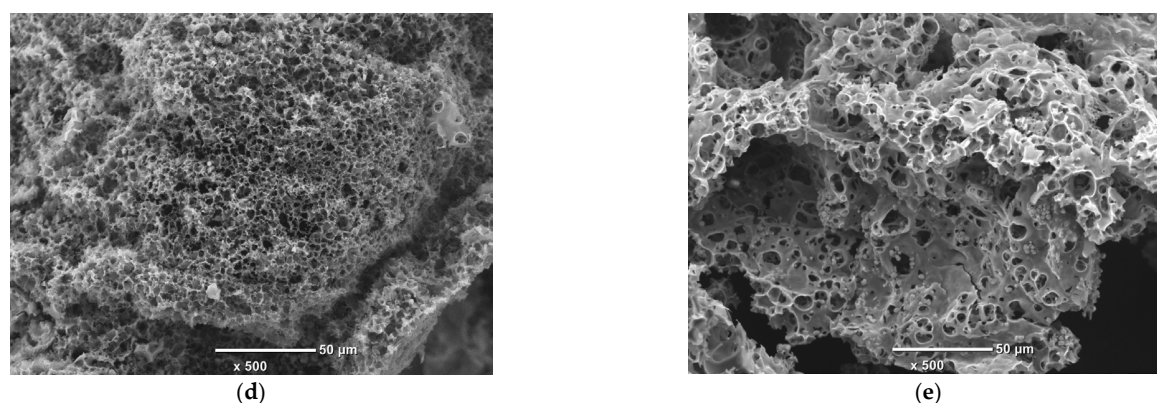(a)   (b)   (c)

Figure 1. *Cont.*

Figure 1. SEM images of unmodified UDLs (**a**), H_2SO_4-modified UDLs (**b**); H_2SO_4-modified UDLs after adsorption (**c**), and TUDL500 (**d**,**e**).

2.1.2. N_2-BET Analysis

The N_2-BET analysis (Table 1) shows that chemical modification and pyrolysis significantly improve the adsorption properties of UDLs. The unmodified UDLs exhibit a low specific surface area ($0.4659 \ m^2 \cdot g^{-1}$), which increases slightly after H_2SO_4 modification ($1.0157 \ m^2 \cdot g^{-1}$). Pyrolysis at 500 °C (TUDL500) dramatically enhances the specific surface area ($451.9304 \ m^2 \cdot g^{-1}$) and creates a microporous structure, making it effective for heavy metal adsorption.

Table 1. BET specific surface area, pore size, and pore volume of unmodified and H_2SO_4-modified UDLs.

UDLs	BET Specific Surface Area ($m^2 \cdot g^{-1}$)	Pore Volume ($cm^3 \cdot g^{-1}$)	Pore Size (nm)
Unmodified	0.4659	0.00092	7.89508
H_2SO_4-modified	1.0157	0.00397	15.63720
TUDL500	451.9304	0.252627	2.23598

2.1.3. XPS Spectra

Unmodified UDLs (a), H_2SO_4-modified UDLs (b), and those after the adsorption of heavy metals (c) were analyzed using XPS, as shown in Figure 2 and Table 2. In the unmodified UDLs, the primary elements detected were carbon (81.04%), nitrogen (2.79%), oxygen (13.74%), and a small presence of calcium (1.59%). Upon modification with sulfuric acid, significant changes in surface chemistry were observed: sulfur appeared at 1.4%, and calcium increased to 3.38%. This indicates the successful incorporation of sulfonate and calcium groups, which is consistent with the sulfonation reaction expected from H_2SO_4 treatment.

After adsorption, XPS spectra showed peaks for Pb4f, Cu2p, Cd3d, and Zn2p, confirming heavy metal binding to the modified UDL surface (Figure 3). The reduction in sulfur (from 1.4% to 0.35%) and calcium (from 3.38% to 0.13%) suggests their involvement in metal binding, likely via ion exchange. The data indicate that adsorption occurs through multiple mechanisms: chemisorption, evidenced by binding energy shifts and strong interactions with sulfonate and hydroxyl groups; ion exchange, as shown by the displacement of sulfur and calcium; and complexation, supported by an increased oxygen content facilitating metal–ligand formation.

In addition, XRD patterns are presented in the Supplementary Information (Figure S2).
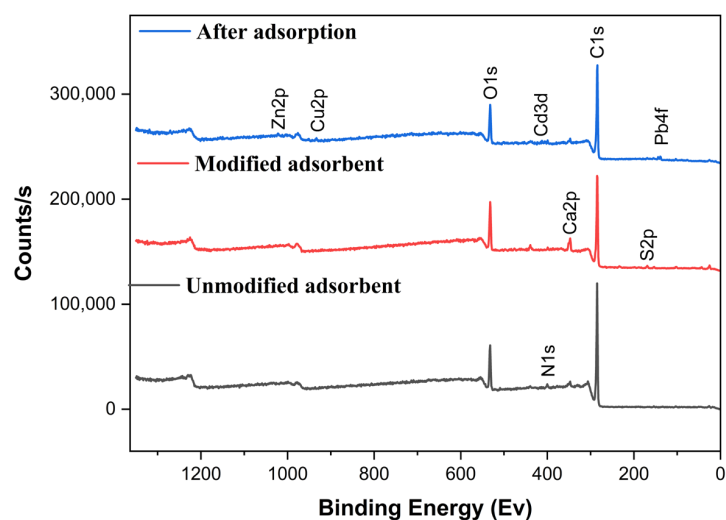
Figure 2. The XPS images of unmodified UDLs, H_2SO_4-modified UDLs, and after the adsorption of heavy metals.

Table 2. The chemical composition of UDLs determined using XPS.

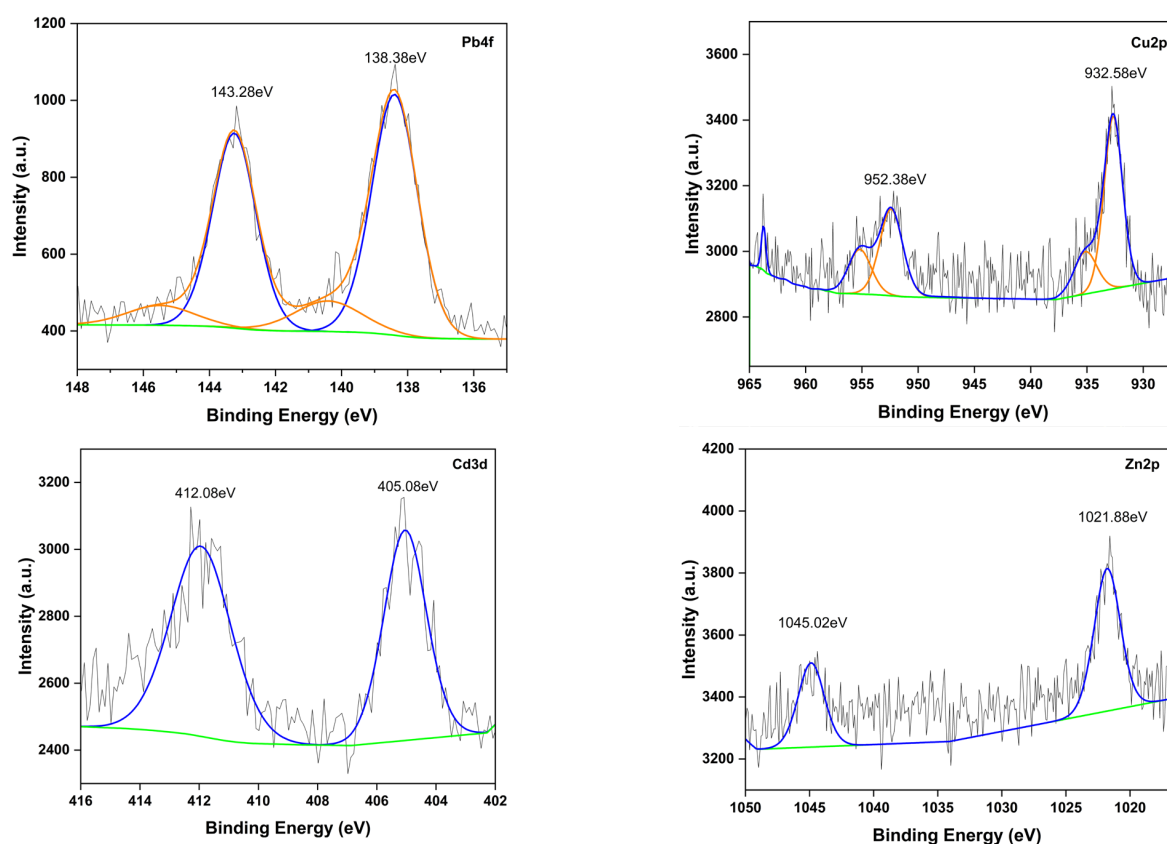| UDLs	C	N	O	S	Ca
Unmodified (%)	81.04	2.79	13.74	-	1.59
Modified (%)	74.97	2.02	16.47	1.4	3.38
After adsorption (%)	80.46	2.88	14.19	0.35	0.13

Figure 3. The XPS spectra after the adsorption of heavy metals. The colored lines represent the peak components obtained from peak fitting. In each spectrum, the blue and orange lines correspond to the deconvoluted peaks: Pb $4f_{7/2}$ and Pb $4f_{5/2}$ for Pb 4f, Cu $2p_{3/2}$ and Cu $2p_{1/2}$ for Cu 2p, Cd $3d_{5/2}$ and Cd $3d_{3/2}$ for Cd 3d, and Zn $2p_{3/2}$ and Zn $2p_{1/2}$ for Zn 2p.

2.1.4. FT-IR Spectra

The FT-IR spectrum of unmodified UDLs, H_2SO_4-modified UDLs, and after the adsorptions of heavy metals is shown in Figure 4. In the spectrum, the broad and strong bands at $3200–3500\ cm^{-1}$ are attributed to hydroxyl (O–H) groups of the biomass. The 2927 and $2853\ cm^{-1}$ peaks correspond to the aliphatic group (C–H, CH_2) stretching vibrations [45]. The peak at $1646\ cm^{-1}$ indicates the C=O stretching vibration of carboxylic acid or other carbonyl-containing groups [46]. The observed peak at $1422\ cm^{-1}$ shows the presence of calcite ($CaCO_3$) [47]. The broad peak at $1059\ cm^{-1}$ is assigned to (C–O, CC, CH_2) from lignin or hemicellulose [48]. After modification, peak intensities at $3200–3500\ cm^{-1}$ are decreased due to degradation of the hydrogen bond between the cellulose chain during the hydrolysis process. Moreover, new peaks at $1162\ cm^{-1}$ (the glucopyranoside ring stretching), $675\ cm^{-1}$, and $615\ cm^{-1}$ (S=O) functional groups were formed [49]. The peak at $1380\ cm^{-1}$ corresponds to the symmetric bending vibrations of methyl groups (CH_3), characteristic of aliphatic hydrocarbons. This sharp peak suggests the presence of organic components in *Urtica dioica*, which may be modified during treatment. While CH_3 groups do not directly bind heavy metals, changes in intensity or shape after adsorption may indicate structural alterations in nearby functional groups [50]. After the adsorption of Pb(II), Cu(II), Cd(II), and Zn(II), the peaks at $3362\ cm^{-1}$ (−OH and −COOH groups), $2927\ cm^{-1}$ (−CH_3), and $1646\ cm^{-1}$ (C=O or −COOH) decreased due to the interaction between the heavy metal molecules and functional groups on the surface of the modified adsorbent [51,52]. Meanwhile, the area of these peaks at $1422\ cm^{-1}$ ($CaCO_3$), $1162\ cm^{-1}$ (the glucopyranoside ring stretching), $1059\ cm^{-1}$ (C–O, CC, CH_2), $675\ cm^{-1}$, and $615\ cm^{-1}$ (S=O) disappeared completely, demonstrating that these groups also participated in metal adsorption [45,51,53]. The $400–540\ cm^{-1}$ peaks indicate the formation of M-O bonds resulting from interactions between metal ions (Pb(II), Cu(II), Cd(II), Zn(II)) and oxygen-containing functional groups (hydroxyl, carboxyl, sulfate) on the adsorbent surface. Moreover, the FTIR spectra of H_2SO_4-modified UDLs (with various concentrations of H_2SO_4) are presented in the Supplementary Information (Figure S4) in more detail.
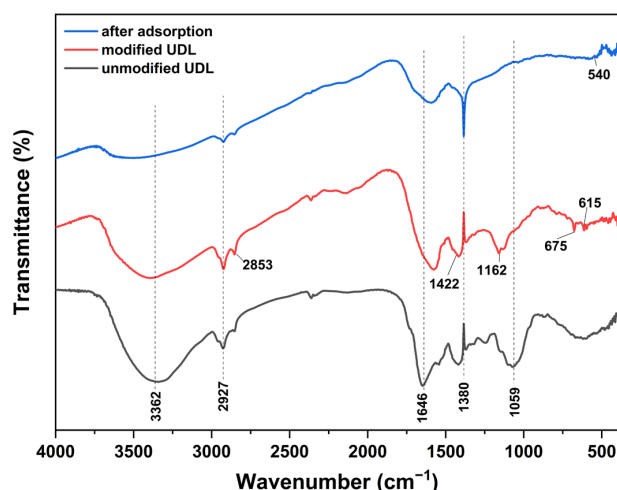

Figure 4. FT−IR of UDLs, H_2SO_4-modified UDLs, and those after the adsorption of heavy metals.

2.2. Evaluation of Multi-Heavy-Metal Adsorption Performance

2.2.1. Effect of Sulfuric Acid Concentration

To determine the modification effect of the sulfuric acid concentration on the adsorption of multiple heavy metals, the sulfuric acid concentration was changed (0–98%), and other conditions remained unchanged (temperature: 298 K, pH: 6, contact time: 2 h, adsorbent dosage: 2 g/L, initial concentration: 50 mg/L). The results are shown in Figure 5. The figure shows that the chemically modified UDLs were able to absorb higher amounts

of Pb(II), Cu(II), Cd(II), and Zn(II) than the unmodified UDLs. For the acid concentration of 40 -H_2SO_4, more than 90% of all four heavy metals was adsorbed simultaneously, and when the acid concentration was greater than 40% H_2SO_4, the adsorption amount decreased slowly. This phenomenon may occur because, when exceeding concentrations of 40% H_2SO_4, the adsorbent can become over-processed, leading to the deterioration or loss of functional groups, as depicted in Figure S4 of the Supplementary Information. Additionally, excessive acid might damage the surface structure or reduce the availability of active sites for metal binding, ultimately decreasing adsorption efficiency [54]. Therefore, in this study, a 30% H_2SO_4 concentration was chosen for the following experiments.
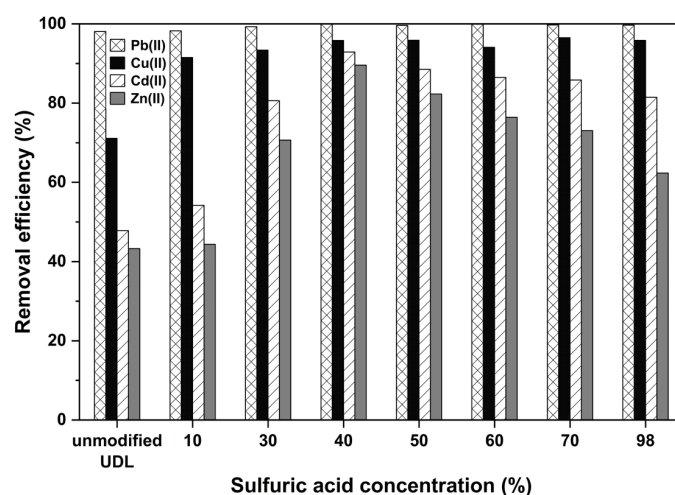

Figure 5. The effect of sulfuric acid concentration on the adsorption of multiple heavy metals.

2.2.2. Effect of Initial pH

The pH value of the aqueous solution can influence the surface charge and metal-binding sites of the adsorbent, as well as the ionization state and form of metal ions [55]. Generally, under high-pH conditions, multiple heavy metal ions form hydroxide precipitates. Therefore, in this experiment, pH tests were performed in the pH range of 1–6. The other adsorption conditions were the same as those in the former (2.2.1) experiment. As shown in Figure 6, the removal efficiency (%) increases with the pH value and reaches a maximum around pH 6. The removal efficiencies at pH 6 were determined as 99.2%, 95.3%, 83%, and 71.6% for Pb(II), Cu(II), Cd(II), and Zn(II) ions, respectively. Therefore, further adsorption experiments were conducted at pH 6. In this study, the zeta potential of H_2SO_4-modified UDLs was measured to investigate the surface charge of the material, and the results are shown in the Supplementary Information (Figure S5).
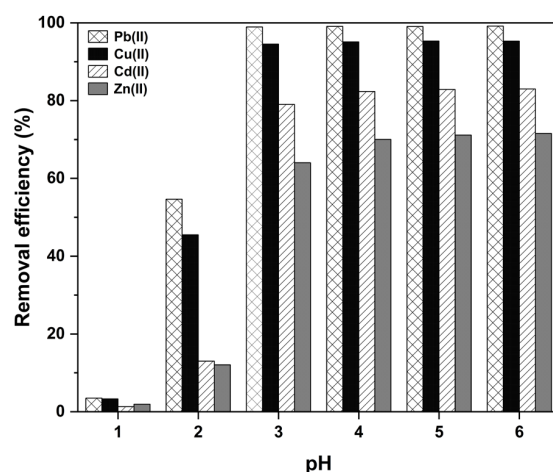

Figure 6. The effect of pH on the adsorption of multiple heavy metals by modified UDLs.

Effects of the adsorbent time and dosage on multi-heavy-metal adsorption performance are also presented in the Supplementary Information (Figure S7).

2.2.3. Effect of Heat Treatment

Figure 7 shows the effect of calcination temperatures (300 °C, 400 °C, and 500 °C) on the adsorption capacities of Pb(II), Cu(II), Cd(II), and Zn(II) using H_2SO_4-modified UDLs. The results indicate that increasing the pyrolysis temperature enhances the adsorption capacities for all metals. The adsorption capacities were 46.6 mg/g, 37.1 mg/g, 11.9 mg/g, and 10.6 mg/g for Pb(II), Cu(II), Cd(II), and Zn(II), respectively, at 500 °C.
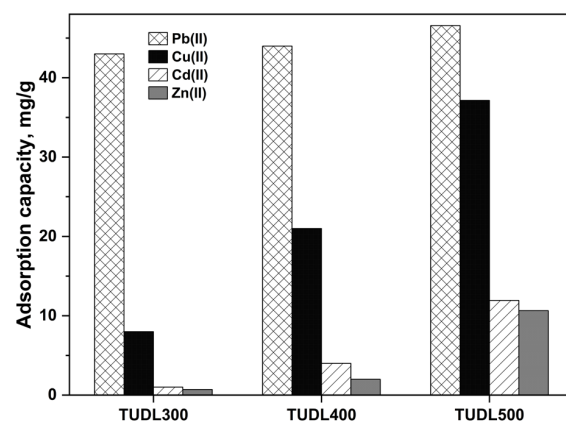

Figure 7. The effect of roasting temperatures on the adsorption of multiple heavy metals.

2.2.4. Effect of Competitive Ions

The effect of competitive ions on multi-heavy-metal adsorption is shown in Figure 8. In this experiment, the adsorption of multiple heavy metals was investigated under the presence of solutions with different concentrations (i.e., 0, 10, 25, 50, and 100 ppm) of each individual (Na^+, K^+, Ca^{2+}, Mg^{2+}) and their complex ($Na^+ + K^+ + Ca^{2+} + Mg^{2+}$). The diagram shows that the adsorption capacities of modified UDLs for multiple heavy metals decrease slightly as the concentration of competing ions increases. However, no notable decrease in the adsorption capacity was observed. This shows that even with a high concentration of competing ions, modified UDLs also show a good adsorption capacity for multiple heavy metals and can be used as an effective adsorbent [55]. Lead (Pb^{2+}) ions, with a larger ionic radius and lower hydration energy than zinc (Zn^{2+}) ions, are more easily attracted to the adsorbent's surface, readily occupying adsorption sites. This is due to their easier dehydration and higher affinity for functional groups (e.g., carboxyl, hydroxyl) on the modified adsorbent compared to Cu^{2+}, Cd^{2+}, and Zn^{2+} ions [56,57].
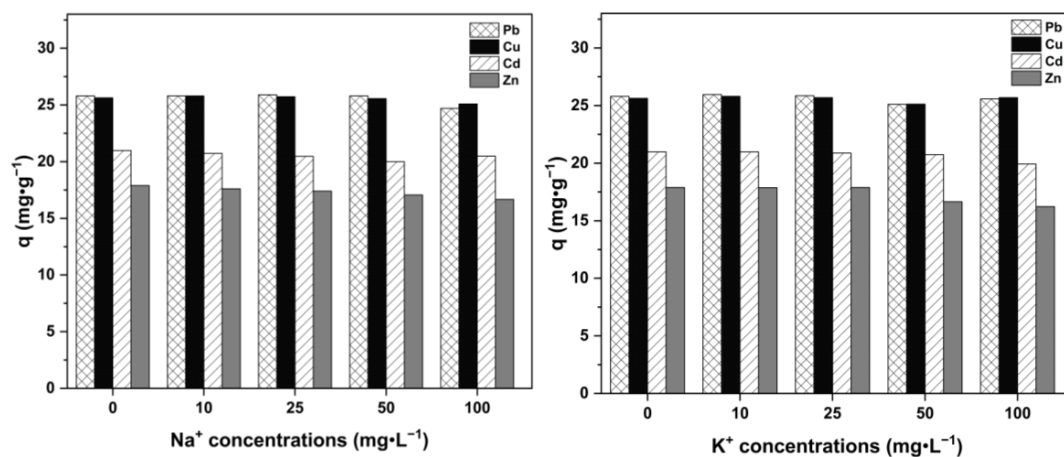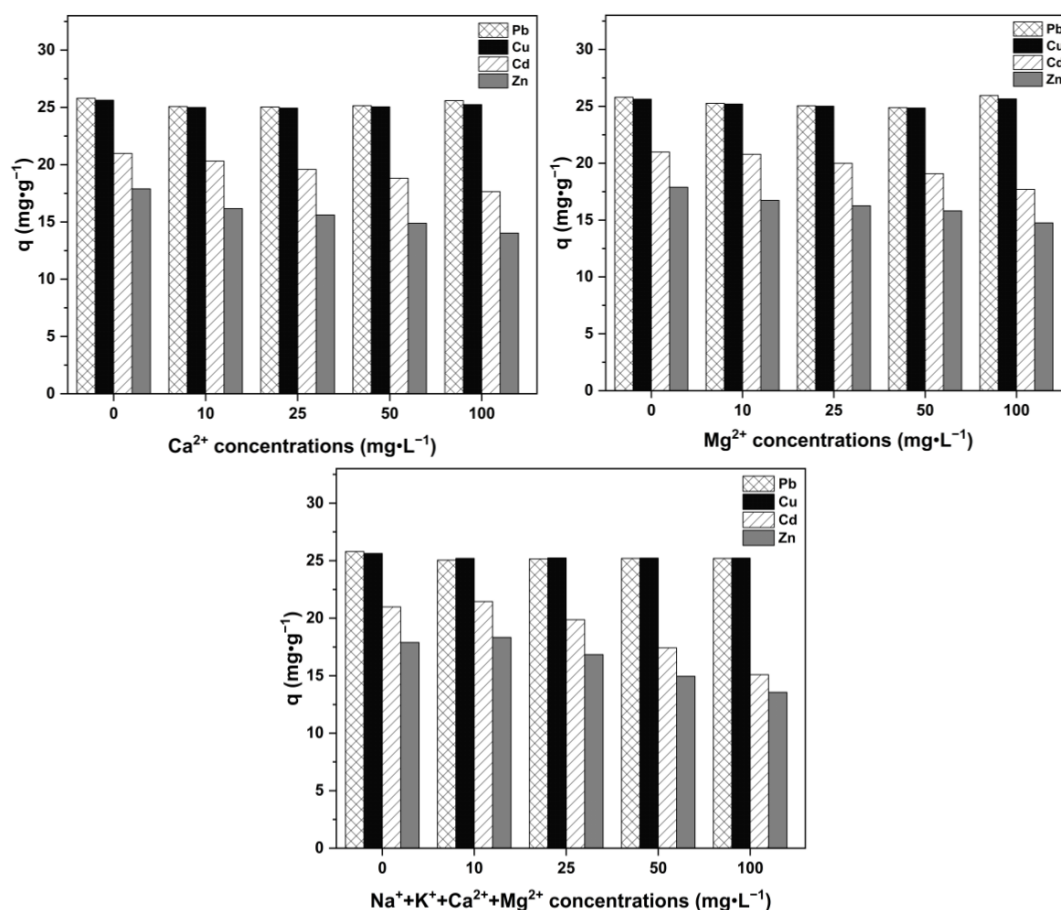

Figure 8. *Cont.*

Figure 8. The effect of competitive ions on the adsorption of multiple heavy metals by modified UDLs.

2.3. Adsorption Kinetics Study

Kinetic investigation of the adsorption process reveals the rate and mechanism of the reaction. These were studied by fitting the experimental data to the pseudo-first-order (PFO) reaction equation and pseudo-second-order (PSO) reaction equation in their linear and non-linear forms. The kinetic equations are described in more detail in adsorption kinetic and isotherm models in Table S2 in the Supplementary Information.

The influence of the contact time on heavy metal adsorption onto modified UDLs was assessed because the adsorption rate and kinetics are crucial for batch-biosorption experiments. The effect of the contact time in the range of 0–15 h for the adsorption of Pb(II), Cu(II), Cd(II), and Zn(II) on the surface of modified UDLs was investigated at a constant pH (=6), constant dosage (2 g/L), constant initial concentration (50 mg/L), and in the range of 298 K. The results are shown in Figure 9 and Table 3, as well as Figures S6 and S8 and Table S3 in the Supplementary Information. The uptake was quick at the beginning because there are many accessible binding sites on the surface of modified UDLs. The equilibrium state was reached at 3 h for heavy metal adsorption. Since the removal efficiencies did not change much after the equilibrium state, further adsorption experiments were conducted for heavy metals at this contact time (3 h).

In Table 3, it is demonstrated that the PSO model generally exhibited superior correlation coefficients compared to the PFO model, although the PFO model is also fit for Pb(II). Additionally, the equilibrium adsorption capacities (q_e) predicted by the PSO model were in closer agreement with the experimental values for all metal ions, indicating that chemisorption is the predominant rate-controlling mechanism.
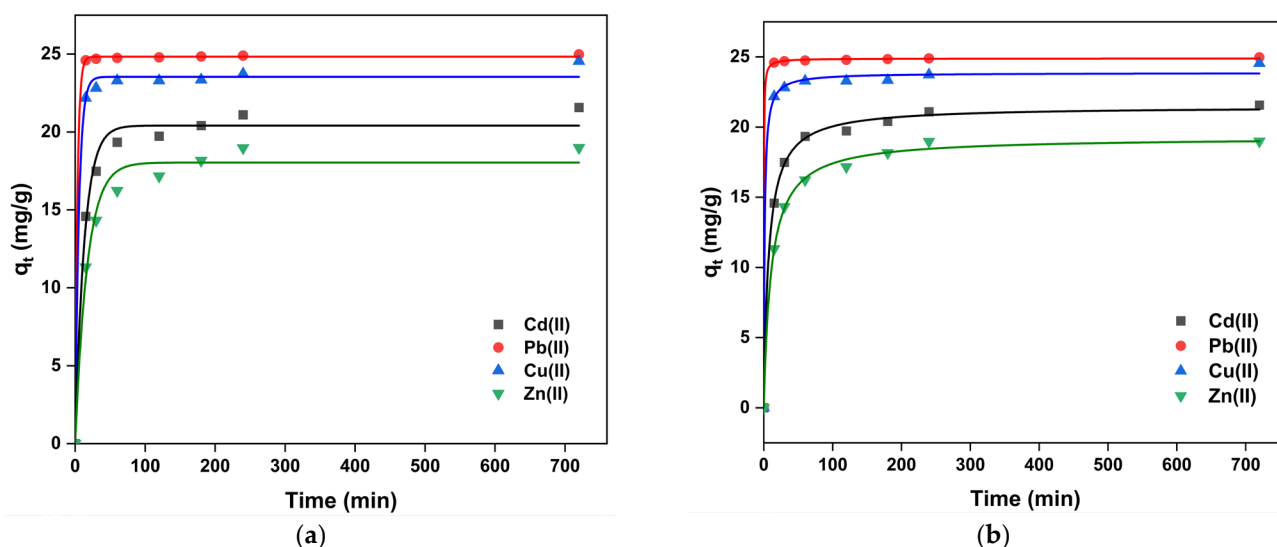
Figure 9. Pseudo-first-order non-linear kinetic models (**a**) and pseudo-second-order non-linear kinetic models (**b**) of multi-heavy-metal adsorption on the modified UDLs.

Table 3. The parameters for the two kinetic non-linear models of adsorption of multiple heavy metals by modified UDLs.

	Pb(II)	Cu(II)	Cd(II)	Zn(II)
		Pseudo-First-Order Model		
q_e (mg·g^{-1})	24.83	23.54	20.41	18.04
K_1 (min^{-1})	0.31	0.18	0.07	0.06
R^2	0.9999	0.9966	0.9882	0.9820
		Pseudo-Second-Order Model		
q_e (mg·g^{-1})	24.89	23.87	21.47	19.27
K_2 (g mg^{-1} min^{-1})	0.20	0.04	0.007	0.005
R^2	0.9999	0.9983	0.9985	0.9979
$q_{e\,exp}$ (mg·g^{-1})	25.52	25.64	22.52	20.90

2.4. Adsorption Isotherm Study

Adsorption isotherms are necessary to understand the adsorption process and predict the adsorption behavior of pollutants onto the adsorbent surface. To evaluate the adsorption data, Langmuir and Freundlich isotherm models were used.

According to the Langmuir isotherm model, the surface of the adsorbent is uniform. During adsorption, each surface molecule or atom of the adsorbent adsorbs a gas molecule, and the gas molecules adsorb on the solid surface as a single layer. There is no force between the gas molecules. This is provided by the following equation:

$$\frac{C_e}{q_e} = \frac{C_e}{q_{max}} + \frac{1}{K_L q_{max}} \tag{1}$$

where C_e and q_e are the heavy metal concentration (mg·L^{-1}) and adsorption capacity (mg·g^{-1}) when the adsorption reaches equilibrium, q_{max} is the maximum adsorption capacity of the adsorbent (mg·g^{-1}), and K_L is the adsorption constant of the Langmuir isotherm (L·mg^{-1}). The relationship between C_e/q_e and C_e gives a straight line with a slope of $1/q_{max}$ and intercept of $1/(K_L q_{max})$.

Freundlich's isotherm model considers multi-layer adsorption without considering the adsorption saturation on multi-layer heterogeneous surfaces. The isotherm of the linear Freundlich model is represented by Equation (4):

$$lnq_e = lnK_F + \frac{1}{n}lnC_e \qquad (2)$$

Among them, K_F is the adsorption capacity $((\text{mg·g}^{-1})·(\text{dm}^{-3}·\text{mg}^{-1})^{1/n})$, and $1/n$ is the adsorption strength. The relationship between lnq_e and lnC_e can be used to determine the $1/n$ and K_F values. The value of $1/n$ can be used to judge the difficulty of the adsorption process: irreversible adsorption ($1/n = 0$), favorable adsorption ($0 < 1/n < 1$), and unfavorable adsorption ($1/n > 1$).

Under the optimal adsorption conditions (pH 6, temperature of 298 K, contact time of 3 h, and adsorbent dosage of 2 mg·L^{-1}), the adsorption isotherm model of modified UDLs for multiple heavy metals was established at the initial concentration of 10–500 mg·L^{-1}. In case of the Langmuir model and Freundlich model (Figure 10), linear correlation coefficients (R^2) were determined (Table 4). In this study, we performed error analyses [58], and the results are presented in Table 4. Specifically, χ^2, MPSD, and RMSE values were calculated. The correlation coefficients (R^2) showed that the Langmuir isotherms and Freundlich isotherms could describe the adsorption of multiple heavy metals well. Although both Langmuir isotherm models and Freundlich isotherm models could express the adsorption of multiple heavy metals on modified UDLs well, the correlation coefficient of the Langmuir isotherm models was higher, indicating that the adsorption of multiple heavy metals by modified UDLs was more in line with the Langmuir isotherm models. The results showed that the adsorption of multiple heavy metals by modified UDLs mainly occurred through a single-layer reaction. Based on the model, the maximum adsorption capacities were estimated to be 98.3 mg·g^{-1} (Pb(II)), 73.4 mg·g^{-1} (Cu(II)), 12.9 mg·g^{-1} (Cd(II)), and 13.9 mg·g^{-1} (Zn(II))).

We also determined non-linear Langmuir and Freundlich isotherms of multi-heavy-metal adsorption, as detailed in the Supplementary Information (Figure S9 and Table S4).
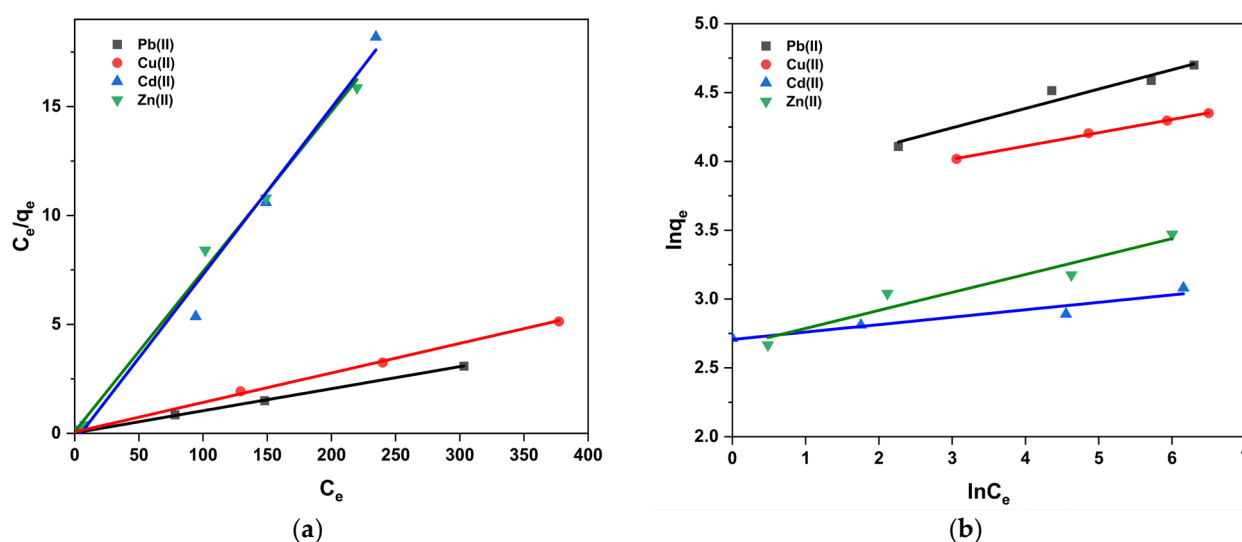

(**a**)   (**b**)

Figure 10. Linear Langmuir (**a**) and Freundlich (**b**) isotherms of multi-heavy-metal adsorption on modified UDLs.

Table 4. The coefficient of linear Langmuir and Freundlich isotherms for multiple heavy metals.

	Pb(II)	Cu(II)	Cd(II)	Zn(II)
	Langmuir Equation			
q_{max} (mg·g^{-1})	98.72	73.85	13.06	13.61
K_L (L·mg^{-1})	0.0002	0.001	0.028	0.006
R^2	0.99	0.99	0.98	0.99
χ^2	0.03	0.26	0.01	0.02
MPSD	0.007	0.05	0.12	0.01
RMSE	1.15	3.22	0.04	0.37
	Freundlich Equation			
R^2	0.93	0.99	0.63	0.63
$1/n$	0.14	0.10	0.05	0.13
K_F (mg·g^{-1})	45.69	41.54	14.97	14.26
χ^2	60.55	24.51	0.28	0.01
MPSD	28.47	19.43	2.68	0.07
RMSE	1500.21	986.15	4.01	0.03
$q_{max,exp}$ (mg·g^{-1})	98.29	73.45	12.90	13.87

2.5. Adsorption Thermodynamics

Thermodynamic tests were performed with the temperature changing between 298 K and 328 K. This study was conducted by changing the temperature (298, 308, 318, 328 K) and keeping all other parameters unchanged. The results are shown in Figure 11. Maximum removal efficiencies at 318 K were determined as 99.2%, 96.4%, 88.7%, and 83.6% for Pb(II), Cu(II), Cd(II), and Zn(II) ions, respectively. Therefore, 318 K was chosen as the most suitable temperature for this study.
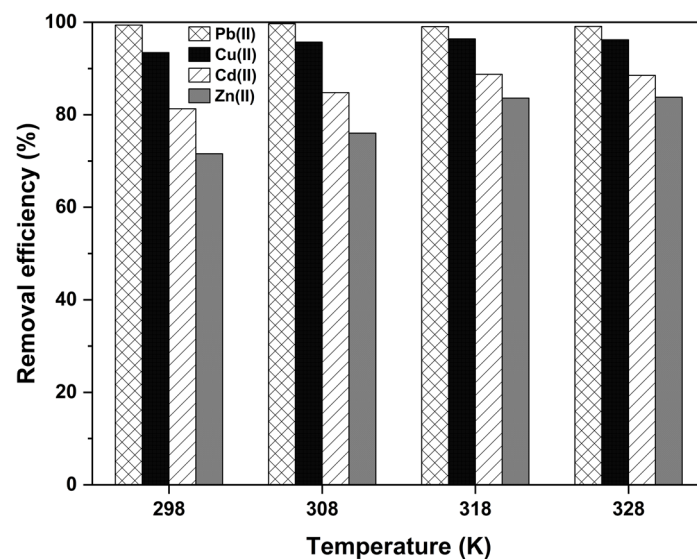
Figure 11. The effect of temperature on the adsorption of multiple heavy metals by modified UDLs.

The thermodynamic parameters for adsorption, including the changes in Gibb's standard free energy ΔG^0 (kJ·mol^{-1}), standard enthalpy ΔH^0 (kJ·mol^{-1}), and entropy ΔS^0 (J·(mol·K)$^{-1}$), were determined (Table 5) using the van Hoff equation [59,60].

$$\Delta G^0 = -RTlnK_c \tag{3}$$

$$lnK_c = -\frac{\Delta H^0}{RT} + \frac{\Delta S^0}{R} \tag{4}$$

where R is the universal gas constant (8.314 J·(mol·K)$^{-1}$) and T is the temperature (K).

The value of K_c can be obtained by $K_c = q_e/C_e$; q_e is the equilibrium adsorption capacity, mg·g^{-1}; and C_e is the equilibrium concentration of Pb(II), Cu(II), Cd(II), and Zn(II), mg·L^{-1}. The slope and intercept of the linear relationship between lnK_c and $1/T$ in Equation (4) were used to calculate ΔH^0 and ΔS^0.

Table 5. The adsorption thermodynamics of multiple heavy metals.

Heavy Metals	C_0, mg·L^{-1}	T, K	ΔH^0, KJ·mol^{-1}	ΔS^0, JK^{-1} mol^{-1}	ΔG^0, KJ·mol^{-1}
Pb(II)		298			−9.85
		308	1.08	36.52	−10.11
		318			−10.48
		328			−10.95
Cu(II)		298			−4.83
		308	19.01	80.76	−6.16
		318			−6.84
	50	328			−7.26
Cd(II)		298			−1.81
		308	18.02	66.91	−2.62
		318			−3.59
		328			−3.68
Zn(II)		298			−0.45
		308	22.95	78.66	−1.17
		318			−2.41
		328			−2.64

Gibbs free energy (ΔG^0) has a negative value, and it tends to be a large negative value with an increasing temperature for all heavy metals, indicating that the adsorption reaction of heavy metals is spontaneous. Given the positive values of the change in enthalpy (ΔH^0), the adsorption process was endothermic for multi-component heavy metals. The positive values of the entropy (ΔS^0) show that irregularity was dominant on the adsorbent surface. From this table, it is suggested that an increased temperature provides additional energy to overcome the activation barrier for adsorption. This indicates that the adsorbent's interaction with heavy metal ions involves energy-intensive processes, likely due to chemisorption, which requires bond formation between the adsorbate and the adsorbent surface. The Langmuir isotherm fit, which indicates monolayer adsorption, was elaborated on by discussing the specific properties of the adsorbent, such as uniform active sites on the UDL surface resulting from sulfuric acid modification [60]. We justified the pseudo-second-order kinetics by linking them to chemisorption mechanisms. This is consistent with the observed adsorption process involving electron sharing or exchange between functional groups on the adsorbent (e.g., sulfonic, calcium, or hydroxyl groups) and metal ions. The discussion also addresses the role of the adsorbent's physical and chemical properties in driving this kinetic behavior.

A comparison of the adsorption capacities of the H$_2$SO$_4$-modified UDLs and TUDLs adsorbents with other previously reported adsorbents is presented in Table 6. As indicated in Table 6, the modified UDLs demonstrated an effective adsorption capacity for multi-component heavy metals compared to other adsorbents from earlier studies. A feature of this research is the identification of a simple and cost-effective method for producing adsorbents.

After calcination, the adsorption capacities did not increase in this study (Figure S10), although the specific surface area of the adsorbent significantly increased, suggesting that other factors might be influencing this outcome. One possible explanation is that heat treatment can damage or reduce the effectiveness of functional groups of H$_2$SO$_4$-modified

UDLs. Therefore, further investigations will be conducted to evaluate the effects of other heat treatment conditions in more detail in future studies.

Table 6. A comparison of the adsorption capacities of modified UDLs with other adsorbents.

Adsorbents	Maximum Adsorption Capacity, q_{max} (mg·g^{-1})				
	Pb(II)	Cu(II)	Cd(II)	Zn(II)	References
Chemically modified dragon fruit peel (DFP)	97.08	-	86.20	-	[39]
Incomplete incinerated *Urtica dioica* leaves (IIN)		46.47		-	[35]
Chemically modified orange peel	73.53	15.27	13.7	-	[61]
Kraft pulp-based carboxymethylated cellulose	20.3	7.8	-	8.4	[62]
Amino-modified wheat straw biochar	46.84	19.79	10.37	-	[51]
Commercial activated carbon (CGAC)	20.3	-	27.3	-	[16]
Unmodified *Urtica dioica* leaves (UDLs)	1.493	1.49	-	1.039	[36]
H$_2$SO$_4$-modified UDLs	98.3	73.4	12.9	13.9	In this study
TUDLs	46.6	37.1	11.9	10.6	In this study

2.6. Chemical Mechanism

The FTIR analysis results confirmed that there were hydroxyl, carboxyl, sulfonate, and Ca^{2+} groups on the adsorbent surface, and the adsorption process was realized through weak interactions, such as electrostatic interactions and hydrogen bonds, through these functional groups. After the adsorption of Pb(II), Cu(II), Cd(II), and Zn(II), the peaks at 3362 cm^{-1} (−OH and −COOH groups), 2927 cm^{-1} (−CH$_3$), and 1646 cm^{-1} (C=O) decreased due to the interaction between the heavy metal molecules and functional groups on the surface of the modified adsorbent. Meanwhile, the area of these peaks at 1422 cm^{-1} (CaCO$_3$), 1162 cm^{-1} (the glucopyranoside ring stretching), 1059 cm^{-1} (C–O, C-C, CH$_2$), 675 cm^{-1}, and 615 cm^{-1} (S=O) disappeared completely, demonstrating that these groups also participated in metal adsorption. From the above results, we surmised that the functional groups (−OH, C−O, the glucopyranoside ring stretching, C=O, and S=O) played an essential role in the adsorption of metals through electrostatic interaction and surface complexation. The XRD analysis showed that calcium crystals were increased after modification, suggesting that calcium ions play a significant role in the adsorption process by participating in ion-exchange reactions during heavy metal adsorption. XPS analysis results indicated the successful adsorption of Pb(II), Cu(II), Cd(II), and Zn(II) by showing the appearance of corresponding peaks for these metals (e.g., Pb 4f, Cu 2p, Zn 2p, and Cd 3d) after adsorption. Furthermore, the analysis indicated that the adsorption mechanism involves ion exchange, as demonstrated by the reduction in calcium content on the adsorbent surface. This ion-exchange mechanism contributes to the efficient removal of heavy metals from aqueous solutions. According to the thermodynamic analysis results, the adsorption processes are spontaneous and endothermic. Overall, the kinetic studies show that the adsorption process included monolayer adsorption and chemisorption mechanisms.

3. Materials and Methods

All chemical reagents, including sulfuric acid, sodium hydroxide, and hydroxyl acid, used in this study were analytical grade and sourced from Kanto Chemical Co., Inc. (Tokyo, Japan). Stock solutions (1000 ppm) of Pb(II), Cu(II), Cd(II), and Zn(II) ions were prepared using Pb(NO$_3$)$_2$, Cu(NO$_3$)$_2$·3H$_2$O, Cd(NO$_3$)·4H$_2$O, and Zn(NO$_3$)$_2$·6H$_2$O in deionized water, respectively. These metal solutions with different concentrations (as required for our experiments) were made by diluting them conveniently. Ultrapure water with a resistivity

of 18.2 MΩ cm (RFU 424TA, Advantech Aquarius, Suite A Dublin, CA, USA) was used in the experiments. In addition, a water bath incubator (BT100, Yamato Kagaku Co., Ltd., Tokyo, Japan), a vacuum drying oven (DP33, Yamato Kagaku Co., Ltd., Tokyo, Japan), and a pH meter (HORIBA F-72, Tokyo, Japan) were used in this work.

Selection of the plant, synthesis of the adsorbent, and thermal treatment of sulfuric acid-modified *Urtica dioica* are outlined in the Supplementary Information (Figure S1 and Table S1). The sample after heat treatment is abbreviated as "TUDL" in the following.

3.1. Characterization of the Adsorbent

The surface functional groups of the adsorbents were identified using Fourier Transform Infrared Spectroscopy (FTIR; FT-IR4200, Jasco, Hachioji, Tokyo, Japan). The FTIR spectra of chemically modified *Urtica dioica* leaves before and after adsorption were obtained in the frequency range of 400–4000 cm^{-1} using the KBr pellet method. X-ray diffraction (XRD) analysis was performed on an X-ray diffractometer (XRD; D2 Phaser, Bruker, Billerica, MA, USA) with Cu-Kα radiation, and the scanning test range was set to 10–70° (diffusion angle). The surface morphology of the materials was observed using scanning electron microscopy (SEM-EDS; JCM-6000 with JED-2300, JEOL, Akishima, Tokyo, Japan) and ion sputtering (JFC1100E, JEOL, Akishima, Tokyo, Japan). The morphologies of unmodified UDLs, modified UDLs, and those after the adsorption of heavy metals were studied using X-ray photoelectron spectroscopy (XPS, K-Alpha, Thermo Scientific Center, Waltham, MA, USA).

3.2. Adsorption Experiments

The adsorption efficiency of the Pb^{2+}, Cu^{2+}, Cd^{2+}, and Zn^{2+} complex solutions with modified UDLs was determined using the following experiments. Initially, adsorption was performed by adding 0.1 g of adsorbent to 50 mL of complex heavy metal solution in a water bath equipped with a heater and shaker. The optimum conditions were determined by conducting adsorption experiments at a 1–6 initial pH, 0–24 h contact time, 0.05–0.20 g/50 mL adsorbent dosage, and 50–500 mg/L heavy metal concentration ranges. The pH of heavy metal solutions was adjusted with 0.1 N of HCl and 0.1 N of NaOH. In our experiments, we used a mixed cellulose ester membrane filter. The filtration time was approximately 3–7 s. The concentrations of heavy metals before and after adsorption in the heavy metal solution were analyzed using inductively coupled plasma atomic emission spectrometry (ICP-AES; SPS1500, SEIKO, Chiba, Japan).

The adsorption capacity, *q* (mg/g), was calculated using the following equation [27]:

$$q = (C_o - C_e) \cdot \frac{V}{m} \tag{5}$$

where C_0 and C_e are the initial and equilibrium heavy metal concentrations (mg·L^{-1}), consecutively; *V* is the volume of solution (L); and *m* is the mass of the adsorbent used (g).

The removal efficiency (*R*) was calculated based on the following equation:

$$R\% = \frac{(C_0 - C_e)}{C_0} \cdot 100 \tag{6}$$

4. Conclusions

Modified *Urtica dioica* leaves (UDLs) were successfully developed as a low-cost and eco-friendly adsorbent for the simultaneous removal of Pb(II), Cu(II), Cd(II), and Zn(II) from aqueous solutions. The physicochemical characterization, including XRD, FTIR, SEM, and XPS, confirmed the structural modifications of UDLs, leading to an enhanced adsorption capacity. Sulfuric acid and heat treatment introduced sulfonate groups, increased

calcium content, and improved the porosity and surface area of the adsorbent, which facilitated metal ion binding through electrostatic interactions and ion exchange. The higher correlation with Langmuir isotherms and pseudo-second-order kinetics indicates monolayer adsorption and predominant chemisorption mechanisms. Maximum removal efficiencies were determined as 99.2%, 96.4%, 88.7%, and 83.6% for Pb(II), Cu(II), Cd(II), and Zn(II) ions, respectively, with optimum conditions at pH 6, 318K, and a 2 g/L adsorbent dosage. Given the positive values of the change in enthalpy (ΔH^0), the adsorption process was endothermic for multi-component heavy metals. Overall, this study demonstrates that sulfuric acid and heat-treated UDLs are an efficient, cost-effective, and sustainable material for removing heavy metals from contaminated water. The findings suggest that they have potential in wastewater treatment, particularly in regions where affordable and accessible solutions are required.

References

1. Peydayesh, M.; Mezzenga, R. Protein nanofibrils for next generation sustainable water purification. *Nat. Commun.* **2021**, *12*, 3248. [CrossRef]
2. United Nations Department of Economic and Social Affairs. *The Sustainable Development Goals Report 2024*; United Nations Publications 2024; United Nations Department of Economic and Social Affairs: New York, NY, USA, 2024.
3. Zhao, M.; Wang, S.; Wang, H.; Qin, P.; Yang, D.; Sun, Y.; Kong, F. Application of sodium titanate nanofibers as constructed wetland fillers for efficient removal of heavy metal ions from wastewater. *Environ. Pollut.* **2019**, *248*, 938–946. [CrossRef]
4. Ijagbemi, C.O.; Baek, M.-H.; Kim, D.-S. Montmorillonite surface properties and sorption characteristics for heavy metal removal from aqueous solutions. *J. Hazard. Mater.* **2009**, *166*, 538–546. [CrossRef] [PubMed]
5. Demey, H.; Vincent, T.; Guibal, E. A novel algal-based sorbent for heavy metal removal. *Chem. Eng. J.* **2018**, *332*, 582–595. [CrossRef]
6. Jaishankar, M.; Tseten, T.; Anbalagan, N.; Mathew, B.B.; Beeregowda, K.N. Toxicity, mechanism and health effects of some heavy metals. *Interdiscip. Toxicol.* **2014**, *7*, 60–72. [CrossRef] [PubMed]
7. Järup, L. Hazards of heavy metal contamination. *Br. Med. Bull.* **2003**, *68*, 167–182. [CrossRef] [PubMed]
8. Qasem, N.A.A.; Mohammed, R.H.; Lawal, D.U. Removal of heavy metal ions from wastewater: A comprehensive and critical review. *npj Clean Water* **2021**, *4*, 36. [CrossRef]
9. Wang, J.; Guo, X. Adsorption kinetics and isotherm models of heavy metals by various adsorbents: An overview. *Crit. Rev. Environ. Sci. Technol.* **2023**, *53*, 1837–1865. [CrossRef]

10. Tran, N.N.; Escribà-Gelonch, M.; Sarafraz, M.M.; Pho, Q.H.; Sagadevan, S.; Hessel, V. Process Technology and Sustainability Assessment of Wastewater Treatment. *Ind. Eng. Chem. Res.* **2023**, *62*, 1195–1214. [CrossRef]

11. Bayuo, J.; Rwiza, M.J.; Sillanpää, M.; Mtei, K.M. Removal of heavy metals from binary and multicomponent adsorption systems using various adsorbents—A systematic review. *RSC Adv.* **2023**, *13*, 13052–13093. [CrossRef]

12. Shen, C.; Zhao, Y.; Li, W.; Yang, Y.; Liu, R.; Morgen, D. Global profile of heavy metals and semimetals adsorption using drinking water treatment residual. *Chem. Eng. J.* **2019**, *372*, 1019–1027. [CrossRef]

13. Bhatnagar, A.; Sillanpää, M. Utilization of agro-industrial and municipal waste materials as potential adsorbents for water treatment—A review. *Chem. Eng. J.* **2010**, *157*, 277–296. [CrossRef]

14. Thiebault, T. Raw and modified clays and clay minerals for the removal of pharmaceutical products from aqueous solutions: State of the art and future perspectives. *Crit. Rev. Environ. Sci. Technol.* **2020**, *50*, 1451–1514. [CrossRef]

15. Septevani, A.A.; Rifathin, A.; Sari, A.A.; Sampora, Y.; Ariani, G.N.; Sudiyarmanto; Sondari, D. Oil palm empty fruit bunch-based nanocellulose as a super-adsorbent for water remediation. *Carbohydr. Polym.* **2020**, *229*, 115433. [CrossRef]

16. Khan, Q.; Zahoor, M.; Salman, S.M.; Wahab, M.; Khan, F.A.; Gulfam, N.; Zekker, I. Removal of Iron(II) from Effluents of Steel Mills Using Chemically Modified *Pteris vittata* Plant Leaves Utilizing the Idea of Phytoremediation. *Water* **2022**, *14*, 2004. [CrossRef]

17. Adeniyi, A.G.; Ighalo, J.O. Biosorption of pollutants by plant leaves: An empirical review. *J. Environ. Chem. Eng.* **2019**, *7*, 103100. [CrossRef]

18. Jayan, N.; Bhatlu M, L.D.; Akbar, S.T. Central Composite Design for Adsorption of Pb(II) and Zn(II) Metals on PKM-2 *Moringa oleifera* Leaves. *ACS Omega* **2021**, *6*, 25277–25298. [CrossRef]

19. Candido, I.C.M.; Soares, J.M.D.; de Araujo Barros Barbosa, J.; de Oliveira, H.P. Adsorption and identification of traces of dyes in aqueous solutions using chemically modified eggshell membranes. *Bioresour. Technol. Rep.* **2019**, *7*, 100267. [CrossRef]

20. Cholico-González, D.; Ortiz Lara, N.; Fernández Macedo, A.M.; Chavez Salas, J. Adsorption Behavior of Pb(II), Cd(II), and Zn(II) onto Agave Bagasse, Characterization, and Mechanism. *ACS Omega* **2020**, *5*, 3302–3314. [CrossRef]

21. Nguyen, D.T.C.; Tran, T.V.; Kumar, P.S.; Din, A.T.M.; Jalil, A.A.; Vo, D.N. Invasive plants as biosorbents for environmental remediation: A review. *Environ. Chem. Lett.* **2022**, *20*, 1421–1451. [CrossRef]

22. Arce, C.; Kratky, L. Mechanical pretreatment of lignocellulosic biomass toward enzymatic/fermentative valorization. *iScience* **2022**, *25*, 104610. [CrossRef]

23. Singh, R.; Kumar, R.; Sarangi, P.K.; Kovalev, A.A.; Vivekanand, V. Effect of physical and thermal pretreatment of lignocellulosic biomass on biohydrogen production by thermochemical route: A critical review. *Bioresour. Technol.* **2023**, *369*, 128458. [CrossRef]

24. Singh, P.; Sharma, S.; Singh, K.; Singh, P.K.; Chowdhury, F.I.; Yahya, M.Z.A.; Yusuf, S.N.F.; Diantoro, M.; Latif, F.A.; Singh, N.B. Recent development on neem (*Azadirachta indica*) biomass absorbent: Surface modifications and its applications in water remediation. *Chem. Phys. Impact* **2024**, *9*, 100773. [CrossRef]

25. Hokkanen, S.; Bhatnagar, A.; Sillanpää, M. A review on modification methods to cellulose-based adsorbents to improve adsorption capacity. *Water Res.* **2016**, *91*, 156–173. [CrossRef] [PubMed]

26. Guo, Z.; Fan, Y.; Liu, T.; Zhang, Y.; Wan, Q. Adsorption and enrichment of Ag(I) from industrial wastewater using woody biomass-based biosorbent. *Hydrometallurgy* **2023**, *219*, 106083. [CrossRef]

27. Feng, S.; Du, X.; Bat-Amgalan, M.; Zhang, H.; Miyamoto, N.; Kano, N. Adsorption of REEs from Aqueous Solution by EDTA-Chitosan Modified with Zeolite Imidazole Framework (ZIF-8). *Int. J. Mol. Sci.* **2021**, *22*, 3447. [CrossRef]

28. Bat-Amgalan, M.; Miyamoto, N.; Kano, N.; Yunden, G.; Kim, H.-J. Preparation and Characterization of Low-Cost Ceramic Membrane Coated with Chitosan: Application to the Ultrafine Filtration of Cr(VI). *Membranes* **2022**, *12*, 835. [CrossRef]

29. Zou, M.; Zhang, H.; Miyamoto, N.; Kano, N.; Okawa, H. Adsorption of an Anionic Surfactant (Sodium Dodecyl Sulfate) from an Aqueous Solution by Modified Cellulose with Quaternary Ammonium. *Polymers* **2022**, *14*, 1473. [CrossRef] [PubMed]

30. Shirendev, N.; Bat-Amgalan, M.; Kano, N.; Kim, H.-J.; Gunchin, B.; Ganbat, B.; Yunden, G. A Natural Zeolite Developed with 3-Aminopropyltriethoxysilane and Adsorption of Cu(II) from Aqueous Media. *Appl. Sci.* **2022**, *12*, 11344. [CrossRef]

31. Du, X.; Kishima, C.; Zhang, H.; Miyamoto, N.; Kano, N. Removal of Chromium(VI) by Chitosan Beads Modified with Sodium Dodecyl Sulfate (SDS). *Appl. Sci.* **2020**, *10*, 4745. [CrossRef]

32. Krajewska, A.; Mietlińska, K. Determining the Parameters of the Stinging Nettle (*Urtica dioica* L.) Hydrolate Distillation Process. *Molecules* **2022**, *27*, 3912. [CrossRef] [PubMed]

33. Antoniadis, V.; Shaheen, S.M.; Stärk, H.-J.; Wennrich, R.; Levizou, E.; Merbach, I.; Rinklebe, J. Phytoremediation potential of twelve wild plant species for toxic elements in a contaminated soil. *Environ. Int.* **2021**, *146*, 106233. [CrossRef] [PubMed]

34. Sharifi, K.; Rahnavard, A.; Saeb, K.; Gholamreza Fahimi, F.; Tavana, A. Ability of *Urtica dioica* L. to adsorb heavy metals (Pb, Cd, As, and Ni) from contaminated soils. *Soil Sediment Contam.* **2023**, *32*, 51–84. [CrossRef]

35. Dimitrijević, V.D.; Stanković, M.N.; Đorđević, D.M.; Krstić, I.M.; Nikolić, M.G.; Bojić, A.L.; Krstić, N.S. The preliminary adsorption investigation of *Urtica dioica* L. biomass material as a potential biosorbent for heavy metal ions. *Stud. Univ. Babes-Bolyai Chem.* **2019**, *64*, 19–39. [CrossRef]

36. Tiwari, P.; Vishwakarma, M.; Joshi, S.; Sharma, H.; Bhandari, N. Adsorption of Pb (II), Cu (II), and Zn (II) Ions onto *Urtica dioica* Leaves (UDL) as a Low Cost Adsorbent: Equilibrium and Thermodynamic Studies. *Mod. Chem.* **2017**, *5*, 11–18. [CrossRef]

37. Isik, B.; Cakar, F.; Cankurtaran, O. Valorization of *Urtica dioica* roots as a highly-effective and eco-friendly biosorbent for adsorptive removal of hazardous textile dyes. *Mater. Sci. Eng. B* **2023**, *293*, 116451. [CrossRef]

38. Viju, S.; Thilagavathi, G.; Vignesh, B.; Brindha, R. Oil sorption behavior of acetylated nettle fiber. *J. Text. Inst.* **2019**, *110*, 1415–1423. [CrossRef]

39. Wattanakornsiri, A.; Rattanawan, P.; Sanmueng, T.; Satchawan, S.; Jamnongkan, T.; Phuengphai, P. Local fruit peel biosorbents for lead(II) and cadmium(II) ion removal from waste aqueous solution: A kinetic and equilibrium study. *S. Afr. J. Chem. Eng.* **2022**, *42*, 306–317. [CrossRef]

40. Joseph, I.V.; Tosheva, L.; Doyle, A.M. Simultaneous removal of Cd(II), Co(II), Cu(II), Pb(II), and Zn(II) ions from aqueous solutions via adsorption on FAU-type zeolites prepared from coal fly ash. *J. Environ. Chem. Eng.* **2020**, *8*, 103895. [CrossRef]

41. Küçük, M.; Makarava, I.; Kinnarinen, T.; Häkkinen, A. Simultaneous adsorption of Cu(II), Zn(II), Cd(II) and Pb(II) from synthetic wastewater using NaP and LTA zeolites prepared from biomass fly ash. *Heliyon* **2023**, *9*, e20253. [CrossRef]

42. Arana Juve, J.-M.; Christensen, F.M.S.; Wang, Y.; Wei, Z. Electrodialysis for metal removal and recovery: A review. *Chem. Eng. J.* **2022**, *435*, 134857. [CrossRef]

43. Dagdag, O.; Quadri, T.W.; Haldhar, R.; Kim, S.-C.; Daoudi, W.; Berdimurodov, E.; Akpan, E.D.; Ebenso, E.E. An Overview of Heavy Metal Pollution and Control. In *Heavy Metals in the Environment: Management Strategies for Global Pollution*; American Chemical Society: Washington, DC, USA, 2023; Volume 1456; pp. 3–24.

44. Zeng, H.; Su, Y.; Gong, X.; Zheng, L.; Zhang, L.; Meng, P.; Zhou, Q.; Ren, J. Competitive adsorption behavior of typical heavy metal ions from acid mine drainage by multigroup-functionalization cellulose: Qualitative and quantitative mechanism. *Environ. Sci. Pollut. Res.* **2023**, *30*, 68191–68205. [CrossRef]

45. Orabi, A.H. Synthesis of a cellulose derivative for enhanced sorption and selectivity of uranium from phosphate rocks prior to its fluorometric determination. *Int. J. Environ. Anal. Chem.* **2019**, *99*, 741–766. [CrossRef]

46. Liu, Z.; Pan, L.; Hu, F.; Hu, Y. Advanced landfill leachate biochemical effluent treatment using Fe-Mn/AC activates $O_3/Na_2S_2O_8$ process: Process optimization, wastewater quality analysis, and activator characterization. *Environ. Sci. Pollut. Res.* **2020**, *27*, 15337–15349. [CrossRef] [PubMed]

47. Ramasamy, V.; Thenpandiyan, E.; Suresh, G.; Sathishpriya, T.; Sagadevan, S. Enhanced electrochemical behavior of naturally derived Eu^{3+}: $PEG/CaCO_3$ nanocomposite for supercapacitor application. *Inorg. Chem. Commun.* **2024**, *159*, 111758. [CrossRef]

48. Orabi, A.; Atrees, M.; Salem, H. Selective preconcentration of uranium on chitosan stearoyl thiourea prior to its spectrophotometric determination. *Sep. Sci. Technol.* **2018**, *53*, 2267–2283. [CrossRef]

49. Hamed, A.; Orabi, A.; Salem, H.; Ismaiel, D.; Saad, G.; Abdelhamid, I.; Elwahy, A.; Elsabee, M. An effective uranium removal using diversified synthesized cross-linked chitosan bis-aldehyde Schiff base derivatives from aqueous solutions. *Environ. Sci. Pollut. Res.* **2023**, *30*, 106790–106811. [CrossRef]

50. Cho, M.-H.; Song, Y.-J.; Rhu, C.-J.; Go, B.-R. Pyrolysis Process of Mixed Microplastics Using TG-FTIR and TED-GC-MS. *Polymers* **2023**, *15*, 241. [CrossRef]

51. Wang, Y.; Zheng, K.; Jiao, Z.; Zhan, W.; Ge, S.; Ning, S.; Fang, S.; Ruan, X. Simultaneous Removal of Cu^{2+}, Cd^{2+} and Pb^{2+} by Modified Wheat Straw Biochar from Aqueous Solution: Preparation, Characterization and Adsorption Mechanism. *Toxics* **2022**, *10*, 316. [CrossRef]

52. Yang, Y.; Chen, N.; Feng, C.; Li, M.; Gao, Y. Chromium removal using a magnetic corncob biochar/polypyrrole composite by adsorption combined with reduction: Reaction pathway and contribution degree. *Colloids Surf. A Physicochem. Eng. Asp.* **2018**, *556*, 201–209. [CrossRef]

53. Fouda, I.M.; El-Kady, M.Y.; El-Sheikh, E.M.; Orabi, A.H.; Youssef, A.O. Elimination of Cr (VI), Pb (II), V (V), and Cd (II) ions from Titanium oxide Pigment from *Rosetta ilmenite* Concentrate Using synthesised Cellulose Phosphorus Oxychloride. *Int. J. Environ. Anal. Chem.* **2023**, *103*, 5795–5814. [CrossRef]

54. Panwar, N.L.; Pawar, A. Influence of activation conditions on the physicochemical properties of activated biochar: A review. *Biomass Convers. Biorefinery* **2022**, *12*, 925–947. [CrossRef]

55. Majigsuren, E.; Byambasuren, U.; Bat-Amgalan, M.; Mendsaikhan, E.; Kano, N.; Kim, H.J.; Yunden, G. Adsorption of Chromium (III) and Chromium (VI) Ions from Aqueous Solution Using Chitosan–Clay Composite Materials. *Polymers* **2024**, *16*, 1399. [CrossRef]

56. Fan, X.; Liu, H.; Anang, E.; Ren, D. Effects of Electronegativity and Hydration Energy on the Selective Adsorption of Heavy Metal Ions by Synthetic NaX Zeolite. *Materials* **2021**, *14*, 4066. [CrossRef]

57. Lee, C.-L.; Hsi, H.-C.; Chang, C.M. Linear correlation between electronegativity and adsorption energy of hydrated metal ions by carboxyl-functionalized single-walled carbon nanotubes. *J. Nanopart. Res.* **2023**, *25*, 59. [CrossRef]

58. Raji, Z.; Karim, A.; Karam, A.; Khalloufi, S. Adsorption of Heavy Metals: Mechanisms, Kinetics, and Applications of Various Adsorbents in Wastewater Remediation—A Review. *Waste* **2023**, *1*, 775–805. [CrossRef]

59. Boparai, H.K.; Joseph, M.; O'Carroll, D.M. Kinetics and thermodynamics of cadmium ion removal by adsorption onto nano zerovalent iron particles. *J. Hazard. Mater.* **2011**, *186*, 458–465. [CrossRef]

60. Mittal, A.; Kaur, D.; Mittal, J. Batch and bulk removal of a triarylmethane dye, Fast Green FCF, from wastewater by adsorption over waste materials. *J. Hazard. Mater.* **2009**, *163*, 568–577. [CrossRef]

61. Lasheen, M.R.; Ammar, N.S.; Ibrahim, H.S. Adsorption/desorption of Cd(II), Cu(II) and Pb(II) using chemically modified orange peel: Equilibrium and kinetic studies. *Solid State Sci.* **2012**, *14*, 202–210. [CrossRef]

62. Islam, M.S.; Rahaman, M.S.; Barbeau, B. Removal of Pb (II), Zn (II), Cu (II), and As (III) ions from water using kraft pulp-based carboxymethylated cellulose in a fixed-bed column adsorption process. *J. Environ. Chem. Eng.* **2023**, *11*, 111181. [CrossRef]